Sensors & Actuators: A. Physical 349 (2023) 114063

Contents lists available at ScienceDirect

Sensors and Actuators: A. Physical

journal homepage: www.journals.elsevier.com/sensors-and-actuators-a-physical

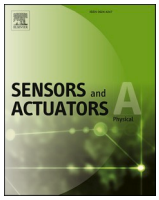

Magnetorheological elastomer-based 4D printed electroactive composite actuators

Mohammadreza Lalegani Dezaki, Mahdi Bodaghi *

Department of Engineering, School of Science and Technology, Nottingham Trent University, Nottingham NG11 8NS, UK

ARTICLE INFO

Keywords:
4D printing
Shape memory polymer
Magnetorheological elastomer
Composite actuator
Magnetic actuation

ABSTRACT

Magnetorheological elastomer (MRE) composite actuators are extraordinary since they can be controlled remotely, move swiftly, adapt to rough surfaces, and engage with humans in a secure manner. Despite all these advantages, pure MREs are not stable enough because of their high degree of softness. Also, a magnetic field is always required to actuate and hold them in the required position accordingly. This paper offers a new conceptual design for bi-stable MRE-based electroactive composite actuators with high performance. The idea is a combination of MRE composites and 4D printing (4DP) of conductive shape memory polymers. The silicone resins are loaded with strontium ferrite magnetic particles and a thin conductive carbon black polylactic acid (CPLA) is 4D printed and embedded as a core inside the composite. A set of parametric studies is carried out to examine the material properties, 4DP characteristics, and magnetization conditions. As an outcome, a functional, lightweight, and bi-stable composite actuator with programmable magnetic patterns is developed. This actuator can be positioned in the actuated situation without any stimuli as long as required. The shape memory behaviour, bi-directionality, and remote controlling of the composite actuator are driven by Joule heating and magnetic fields. The actuator with a weight of 1.47 g can hold and lift weights up to 200 g. Finally, experiments are conducted to demonstrate the immense potential of the developed composite actuators as mechanical and biomedical devices. Due to the absence of similar concepts and results in the specialized literature, this paper is likely to advance the state-of-the-art smart composite actuators with remotely controlled shape-memory features.

1. Introduction

Four-dimensional (4D) printing (4DP) is a cutting-edge technology that was developed and designed to change the shape of the printed parts into artefacts [1–3]. Despite the field's substantial advancement, the manufacturing of static solid objects still restricts its commercial applications. Consequently, with the recently established 4DP technology, innovative materials programmed to change their characteristics, functionalities, as well as their shapes, are created [4,5]. In other words, the inclusion of life into 3D-printed items through the time dimension aids in the development of 4D-printed adaptable products. 4DP technology has many benefits over traditional subtractive manufacturing, including quick prototyping, affordability, accessibility, less material usage, better design flexibility, and geometric complexity [6]. These creative products are constructed from a variety of smart materials.

Smart materials that react to external stimuli in a predictable and controllable way have become more and more in demand in recent years [7,8]. These materials are divided into shape memory polymers (SMPs) [9], shape memory alloys (SMAs) [10], shape memory polymer composites (SMPCs) [11], magneto/electro materials [12], liquid crystal elastomers [13], and hydrogels [14]. Smart materials are space-time dependent and can change over time depending on the external stimuli they are exposed to, such as temperature [15], light [16], pH [17], magnetic field [18], electricity [19], and moisture [20].

The development of macro- and micro-scaled soft robots and actuators for various technical applications has recently made substantial use of 4DP technology [21]. Of all the 4DP methods, fused deposition modelling (FDM) is the most economical and widely used [22]. A potential way to stimulate FDM 4D-printed actuators is thermal activation [23]. By adjusting the printing parameters and heat as the actuation source, numerous shape transformations of 4D-printed components with thermoplastic FDM filaments like polylactic acid (PLA) can easily be accomplished [24]. The use of SMPCs in various fields is significantly impacted by stimuli-responsive approaches. Electroactive SMPCs can restore their shape thanks to the Joule heating effect and are less susceptible to environmental influences [25,26].

* Corresponding author.
E-mail address: mahdi.bodaghi@ntu.ac.uk (M. Bodaghi).

https://doi.org/10.1016/j.sna.2022.114063
Received 16 August 2022; Received in revised form 3 November 2022; Accepted 26 November 2022
Available online 28 November 2022

Many techniques are developed to create electroactive SMPCs [27, 28]. Dong et al. [29] used the FDM process to create electroactive PLA/carbon nanotube-based composites for various smart devices with remote control capabilities. The scientists looked into different SMPC-based complex structures produced in 2D and 3D remembered shapes in response to the electric stimulation. The findings demonstrated that, up to a point, adding carbon nanotube content increases the thermal conductivity, electrical conductivity, and form recovery ratio of SMC. Mitkus et al. [30] outlined bi-layer SMP/conductive PLA (CPLA) structures and tried to enhance their controllability and bending deflection. Results showed a considerable reduction in resistance is produced when various activation voltages are applied to the structure.

Wang et al. [31] provided a novel printed paper actuator as a low-cost, electrically powered, reversible actuation, and sensing technology using CPLA and FDM. Different applications of this developed actuator were outlined to show the capabilities of electroactive polymers. Lee et al. [32] printed four actuators using CPLA at various printing speeds and activated them by Joule heating. They observed an increase in bending as the printing speed rose. Results showed that the actuators were turned on by progressively heating them from 30 °C to 80 °C while allowing an electrical current to flow through them. Also, CPLA can be used in building circuits and electronic products. Flowers et al. [33] illustrated the possibility of employing FDM 3D printing to create a variety of frequently used electronic components separately and printed entire circuits made up of several components in a single phase.

Soft actuators comprising elastomers and gels functionalized with magnetically active materials are obvious options for driving soft robots' magnetically controlled motions. Recent advancements in soft actuator technologies, such as 4DP, origami, tough hydrogels, mechanical metamaterials, electroactive polymer, and liquid metal-injected elastomers, provide the technical framework for creating soft actuators and robots with dramatically improved performance [34]. When an external magnetic field is introduced, magnetorheological elastomers (MREs) with a polymeric matrix and magnetic fillers can have their mechanical properties controlled [35].

Since a magnetic field is a contactless and fast-acting force that is relatively harmless to the human body, applying one seems like a good way to elicit certain responses. Particularly, MRE materials or composites are those that, when subjected to an external magnetic field, display tunable rheological and viscoelastic characteristics, such as shear stress, yield stress, dynamic modulus, and damping [36]. The magnetic resonance (MR) effect is a change in the mechanical properties of a composite caused by the magnetic interaction between particles within the surrounding matrix, which results in the creation of chain-like structures oriented roughly parallel to the magnetic field. Micron-sized particles in the size range of 3–5 μm with magnetic properties that are integrated into a nonmagnetic medium make up the majority of MRE materials [37].

Magnetically responsive actuators are particularly intriguing among the several conceivable types of devices and actuation modes since they are quick, contactless, and powered by magnetic fields that may be used safely around people [38]. Contactless control is essential for minimally invasive medical devices because it enables the manipulation of untethered equipment in small places [39,40]. Recent studies have demonstrated that when an external magnetic field is applied, soft objects with tunable local magnetization patterns can perform sophisticated motions including crawling, rolling, and jumping [41–43]. Soft actuators can be used as soft grippers in different applications as well [44].

The actuation of grasping fingers, the stiffness of encasing MR elastomers and fluids, and the adhesion force between the gripper and the object can all be controlled by an externally generated magnetic field. A magnetic gripper with programmable arm motion managed by an external magnetic field was demonstrated by Xu et al. [42] and Zhang et al. [45]. An electromagnet inserted at the gripper's core was used by Skfivan et al. [46] to regulate the mobility of the beaks which had no joints and fingers. The study used MR elastomers for the beaks and fingers, which could adjust their stiffness and centre of mass by adjusting the magnetomotive force of the electromagnet.

Also, Carpenter et al. [47] developed a soft magnetic actuator using strontium ferrite which could be activated under a low magnetic field. The addition of a neodymium permanent magnet to the middle of the non-adhering side of an elastomeric suction cup by Iwasaki et al. [48] was another intriguing innovation. By manipulating the magnetic field, the authors were able to direct the velocity of the array of suction cups and anchor the array in the appropriate spot. The applied magnetic field also regulated the adhesion and detachment of the suction cup, allowing for complete item manipulation and release.

Despite the various advantages that MRE soft actuators could bring, a magnetic field or permanent magnet should always exist to activate and hold the actuator in the required position. Meanwhile, it has not yet been determined how well electroactive 4DP can work with MRE actuators. The electroactive CPLA and MRE components used in this work are the first to be combined to create a bi-stable, reversible, and lightweight composite actuator. Introduced is a novel composite soft actuator made entirely of CPLA and MRE, powered by permanent magnets, operated at a low magnetic field and activated via the Joule heating technique. This study presents, for the first time, a bi-stable smart soft composite actuator that can be programmed remotely. A combination of magnetic and electric Joule heating stimuli is employed to activate the actuator. As a result, a bi-directional actuator is developed using MRE and 4DP technology.

The main goals of this work are to highlight some important design characteristics, to offer a conceptual design, and to comprehensively describe the manufacturing procedure used to create these kinds of soft shape-memory actuators. A straightforward production process can develop actuators for a variety of applications faster. It is expected that the model and solution techniques will pave the way for creating lightweight MRE-responsive Joule heating actuators that possess high stability and a tiny contact area. This paper is organised as illustrated in Fig. 1. CPLA's mechanical characteristics are investigated. Additionally, details about the electroactive materials and shape-changing effects of 4D-printed CPLA are presented. The details of how MRE composites are integrated with 4D-printed CPLAs are discussed. The application of the developed actuator is then assessed appropriately.

2. Materials and methods

2.1. Materials

A variety of thermoplastic filaments that already exist and may include functional additive particles can be used for FDM 4D printing of objects with different material qualities and multifunctional features. By intentionally altering the print at specific spots, these qualities may be customised across the fabrication. CPLA (Proto-Pasta, Proto Plant, USA) which is an electrically conductive carbon black PLA is used in this study. Also, black polylactic acid (PLA) filament from Creality company is used for DMA mechanical tests accordingly. This is because PLA is affordable, commercially available, and displays a prominent shape memory effect among well-known SMPs. CPLA is a mixture of electrically conductive carbon black (approximately 21 wt %) and PLA. Hence, CPLA is a fantastic option for low-voltage applications such as circuits, touch sensors, and employing prints to interface with touch screens. When the material is heated from room temperature to 80 °C, there is a reported loss of up to 98.6 % in Young's modulus [49]. The microstructure of CPLA and its features are assessed using scanning electron microscopy (SEM) on a JSM-7100 F LV FEG SEM equipment.

The second material is a chemical composition of strontium ferrite, $SrFe_{12}O_{19}$, (UF-S2). The chemical composition, size, and shape of the magnetic particles utilised in the formulation can be varied widely due to the adaptability of the suggested manufacturing method [50]. This design space can be investigated by looking at the magnetic properties,

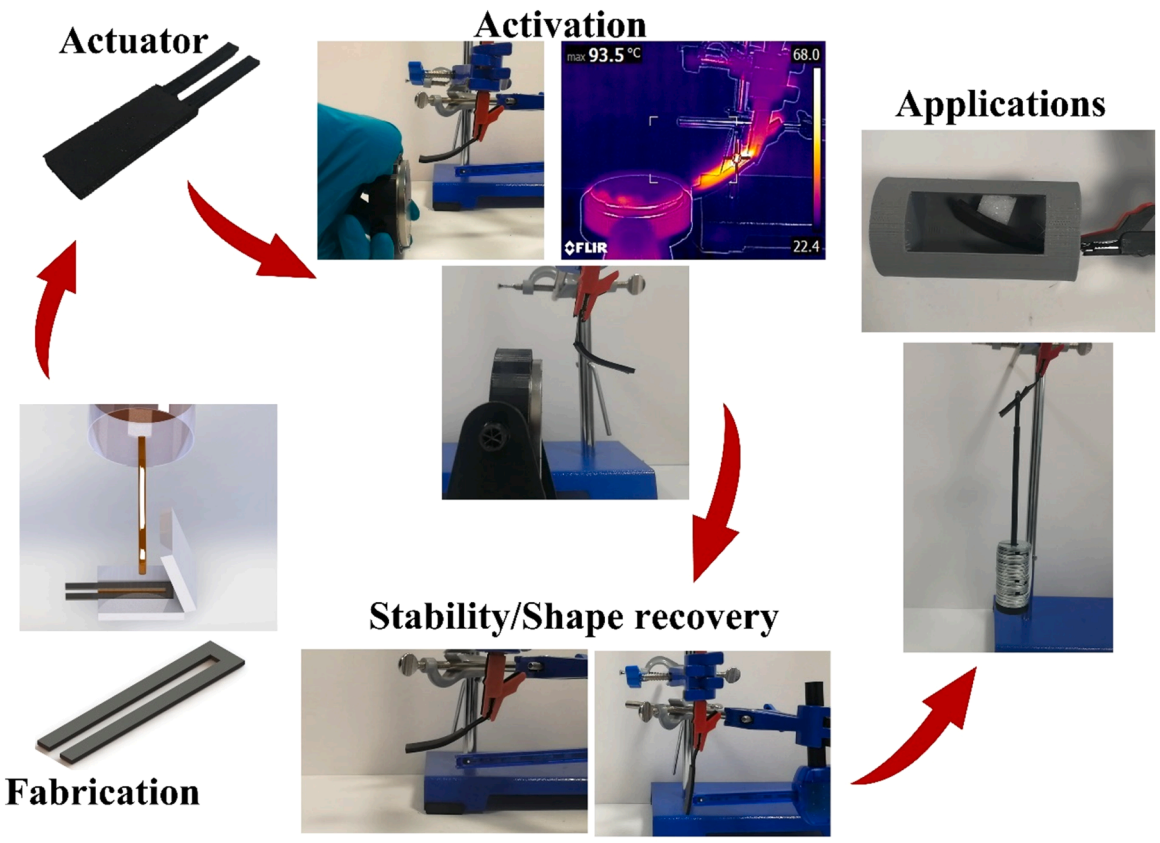

Fig. 1. Schematic steps from fabrication to application of the proposed actuator.

mechanical properties, and deformation of composites created with various kinds of particles. UF-S2 from DOWA Electronics Materials is used and investigated in accordance with its bimodal particle size distribution. It has a compacted density of 3.58 g/cm^3 and an average particle diameter of 1.3 μm. Due to its biocompatibility and ability to be magnetised using composites containing UF-S2 particles at relatively low magnetic fields, this powder is intriguing for the manufacturing of soft actuators [51,52].

2.2. 4D printing procedure

The 4DP of intelligent structures is made possible by the FDM process. The Ultimaker S3 FDM-type 3D printer, which has two 0.4 mm nozzles is used to create all the study's samples. The 3D-printed structure and its design are demonstrated in Fig. 2(a) and (b). The design of the structure focuses on the phase changes of CPLA. This design allows a better heat distribution throughout the structure as reported previously [29,30]. The properties in terms of conductivity and resistance of CPLA have been reported previously [49,53,54]. Also, this design increases the stability of MRE while the weight remains almost the same with the same size. The length of the structure is longer to have better clamping and electrical connections. The hotbed and printing temperatures are set 30 °C and 210 °C, respectively. To maintain internal continuity, the concentric filling approach is used, and the filling rate is set at 100 %. To improve the printing quality, the height of a single layer is set to 0.2 mm and no coating is used. Also, the printing speed is considered 70 mm/s for better actuation behaviour [55]. The structure shapes the core of MRE which increases the stability, and the material's electroactive behaviour is an alternative option to eliminate the magnetic field. The resistance of the CPLA structure is varied by altering the size of the 3D-printed structure. As a result, the structure's temperature distribution will shift and the electrical input current will also need to be

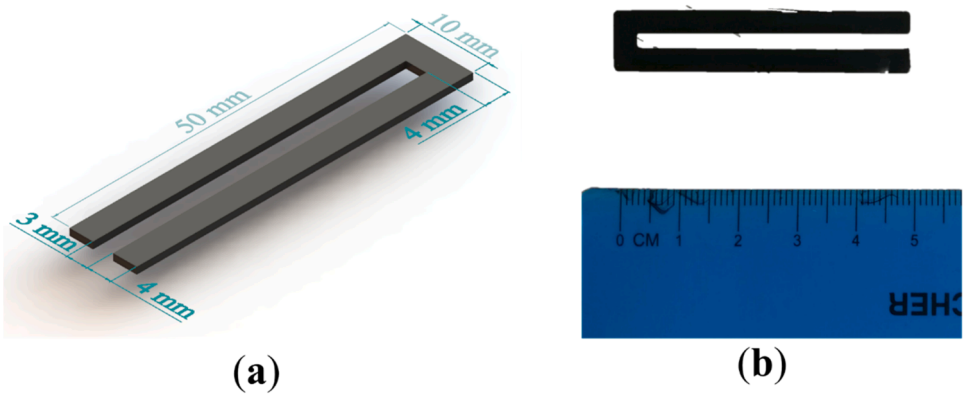

Fig. 2. . (a) 3D schematic and details of 4D-printed structure and (b) 4D-printed core structure.

modified.

2.3. MRE-based 4D-printed composite

MRE soft materials can be used as sensors, actuators and quick, untethered robots for pick-and-place, gripping, and moving activities as well as 3D objects with remote control morphing capabilities [56–58]. The use of MRE with a 4D-printed structure is intended to create the thinnest bi-stable shape memory actuator. The design enables the creation of an actuator based on the required specifications.

Simply mixing magnetic particles with a two-part silicone resin and moulding the resulting viscous paste yields MRE soft actuators. The Ecoflex 00–30 silicone resin (parts A and B) from Smooth-On-Inc. is combined with the UF-S2 particles using an IKA MINISTER stirrer until a smooth, viscous paste is achieved. The composite paste utilised to create all the films is 70 % bimodal UF-S2 particles. The magnetic properties of the composite films are assessed by measuring the magnetic flux density on the surface of the samples in the out-of-plane direction. The paste is moulded into 3D-printed PLA moulds fabricated by the FDM process. The formation of a percolating network between the particles causes the resin to become more viscous, which also prevents the final paste from flowing easily. Therefore, the paste needs to be squeezed throughout the casting process to completely fill the moulds and create a clean surface finish. The high paste viscosity makes it impossible to eliminate the existence of air bubbles, yet they have no appreciable effect on the magnetic actuation properties of the material.

The magnetic silicone composite films are not stable enough and required a magnetic field throughout the procedure. Therefore, it is crucial to keep the actuator in place without affecting its stiffness or weight. To eliminate the magnetic field and reach a stable design, a 4D-printed structure is used as a core layer. The actuators are especially well suited for developing structures with shape memory behaviour and shape recovery capabilities. Composite films are produced using a similar process as shown in Fig. 3. During the curing period, the silicone is placed on the bottom and top of the 4D-printed structure as illustrated in Fig. 3(a) and (b). FDM is used to create the mould, which is then filled with two-part silicone resin and magnetic particles. The magnetic viscous is poured first and then the CPLA structure is placed on the magnetic paste. Then, the viscous paste is poured until a 2.5 mm total thickness of the actuator is attained. A plate is positioned and compresses the MRE-based composite after that. After shaping, the composite is left to cure for at least 4 h at room temperature using a neodymium magnet on one side of the mould (see Fig. 3(c)).

A square neodymium magnet is utilised to provide consistent out-of-plane magnetization. The soft actuators are magnetised during the curing process using permanent magnets that are positioned on one side of the mould. One square magnet (15 ×15×8 mm, N42, Magnet Expert Ltd) is placed at the end of each film to magnetise the MRE-based composite. Samples magnetised during curing achieve a greater degree of magnetization as a result of the particles aligning with their easy axis along the applied field [47]. The final sample is 55 mm long, 12 mm wide, and 2.5 mm thick in size (see Fig. 3(d)). In order to determine how the presence of a 4D-printed structure in the MRE affects stability and weight, samples' behaviours are investigated. The applied magnetic field can be controlled by varying the distance between the magnet and the actuator. The actuators can be stimulated by activating the 4D-printed structure through Joule heating and applying a low magnetic field.

2.4. Dynamic mechanical analysis of 4D-printed structure

Most polymers typically exist in a soft, above-glass transition temperature state, and in a hard, brittle state at ambient temperature. The dynamic mechanical analyser (DMA) 8000 from PerkinElmer is used to test the storage modulus of CPLA and pure PLA from Creality. The sample for the DMA test is produced at a speed of 70 mm/s, and its model measurements are 40 mm in length, 10 mm in width, and 1 mm in thickness. The two most important thermodynamic factors that

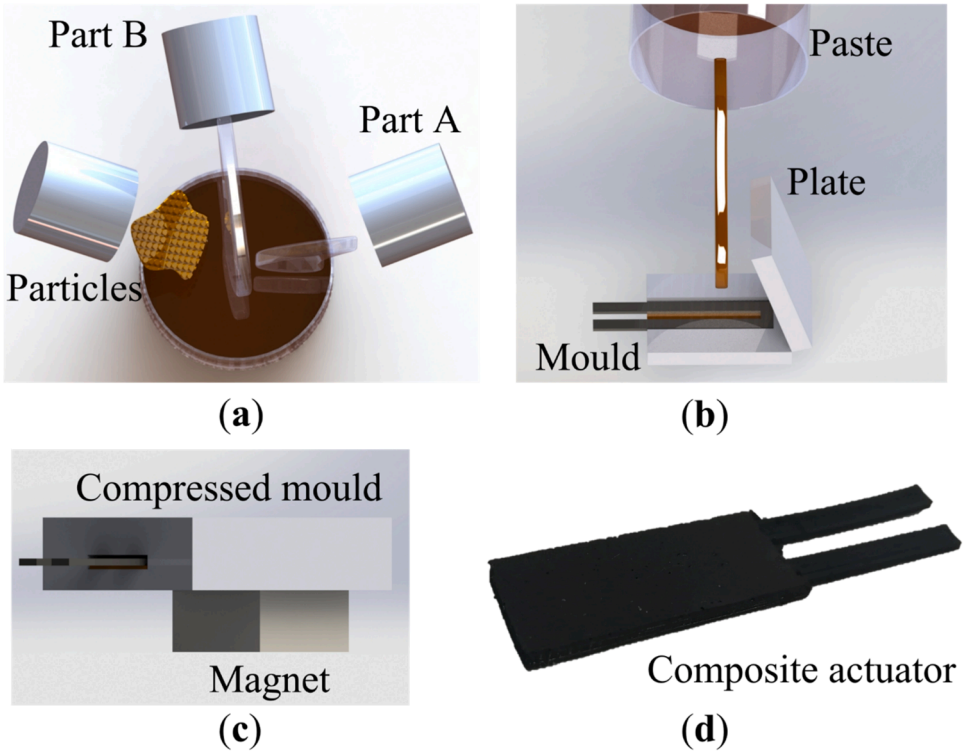

Fig. 3. MRE-based composite manufacturing, magnetization, and activation. (a) Soft paste is produced by mixing the magnetic powder with silicone resins. (b) The viscous slurry is cast into a 3D-printed mould to create actuators with precise geometry. (c) During the curing process, the actuator is magnetised by positioning neodymium magnets in certain spots and compressed until the paste is cured. (d) MRE-based electroactive composite actuator.

contribute to the shape memory effect of SMPs are storage modulus and glass transition temperature (T_g), and, therefore, they should be studied in order to assess the electro-induced shape memory behaviour of 4D-printed CPLA. Additionally, it's important to describe how particle integration affects the storage modulus and T_g of the employed CPLA. The chosen test frequency is 1 Hz, which corresponds to the gradual alteration in characteristics brought on by temperature. The DMA test sequence ramps from a starting temperature of 30–100 °C at a rate of 2 °C/min.

2.5. Electrical connection and measurements

Printed CPLA to the power wires should offer a mechanically reliable connection at both room and working temperatures. An easily breakable connection is also preferred for the majority of applications. The DC power supply provides the necessary electricity. For experimental circuits without additional electrical protection, voltage is restricted to 120 VDC. For semi-permanent or temporary connections in laboratories, crocodile clamps on exposed terminals are typically utilised. The current entering the CPLA structure during activation is measured using a digital multimeter. The data is read by Keithley KickStart Software. The behaviour of the 4D-printed structure is evaluated using an infrared camera from FLIR. To guarantee that the structure is heated above its T_g, the applied voltage is changed from 60 V to 120 V. The cables are linked, a specimen at a time is positioned vertically in the test stand, and the subsequent test process is utilised, see Fig. 4. By employing rectangular strip specimens as the permanent shape, a bending test is used to look at the shape memory behaviours. The shape-fixing method involves applying an external force to deform each specimen to the pre-setting deformation state (U shape) above T_g and maintaining that force after the power is turned off until the specimen is cooled and hardened. In order to attain the maximum recovery, the voltage is then supplied to the specimen one more time. A video camera records the shape recovery behaviour, and metric like recovery time is used to quantify it.

2.6. Magnetic measurement

The hysteresis loops of magneto-responsive composites are seen at 300 K at a rate of 2.5 mT/s using a physical property measurement system (PPMS; Quantum Design). To assess the actuator's reactions, we measure the bending deflection of the free-hanging cantilever composite actuator in the presence of an external lateral magnetic field from the permanent magnet (60 mm diameter and 5 mm thick N42, Magnet Expert Ltd.). The magnetic field strength between the actuator and permanent magnet is evaluated to investigate the behaviour of the actuator. The experiment is run when the composite actuators are subjected to an outside magnetic field and Joule heating activation (see Fig. 4). To control their motion, magnetization patterns are created during the manufacturing process. The magnetic field is measured using a Pasco magnetic field sensor with a probe that has a resolution of 0.01 G at a frequency of 10 Hz. The magnetic strength of the permanent magnet is recorded using PASCO Capstone. Additionally, the magnetic flux density is tested using a portable Gaussmeter from RS Pro. In order to calculate bending angles and deflection, PASCO software records the trajectory trajectories of soft actuators.

2.7. Mechanical properties of MRE

The mechanical characteristics of the composites are evaluated using a universal mechanical testing apparatus (Shimadzu AG-X plus machine). Five samples of the silicone material Ecoflex 00–30 in dog-bone shape and five samples containing 70 wt % magnetic particles with a gauge length of 33 mm in compliance with ASTM D412 are investigated [59]. The test is carried out to compare the stresses under magnetic and non-magnetic conditions. The dog-bone samples are subjected to a 500 mm/min displacement rate while being clamped between jaws.

3. Results and discussions

3.1. Electroactive shape memory performance

The storage modulus and tan δ and loss modulus values from the DMA are shown in Fig. 5(a) and (b). The T_g value for CPLA is close to 75 °C while it is 55 °C for pure PLA [32,49] and the inclusion of carbon black marginally raises the T_g of the composites. It occurs as a result of carbon acting as heterogeneous nucleation locations to raise the PLA matrix's crystallisation temperature. The addition of carbon increases the stiffness of the PLA matrix a bit, resulting in storage moduli of CPLA that are slightly higher than pure PLA. The chain flow causes the materials to lose stiffness and quickly decreases their storage modulus, turning them into a rubbery, viscous liquid form. In contrast, the material's loss modulus rises as a result of increasing molecular friction between its polymer chains, which raises the amount of energy wasted. The loss modulus increases when it is close to the glass transition phase and then falls sharply since the molecular activities decline, and less energy is lost when it is close to the T_g. SEM is used to examine the

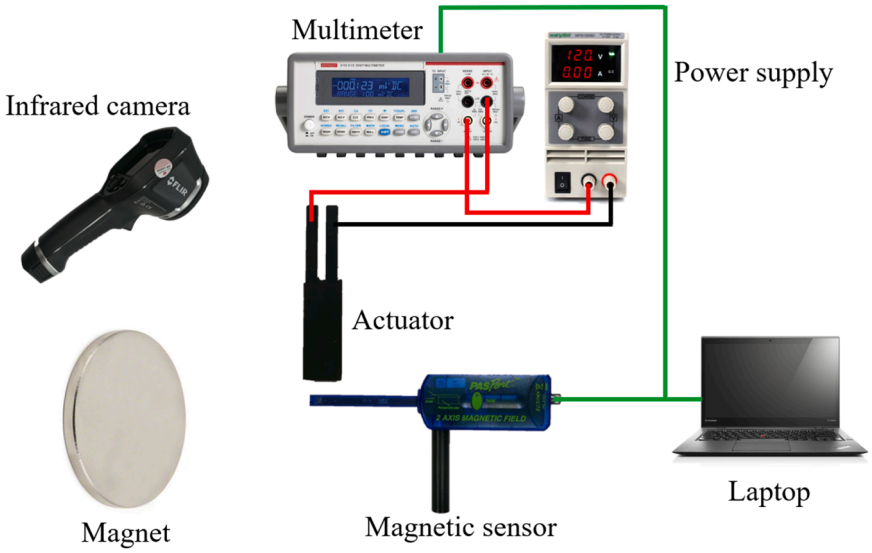

Fig. 4. A schematic of the system and components to record data.

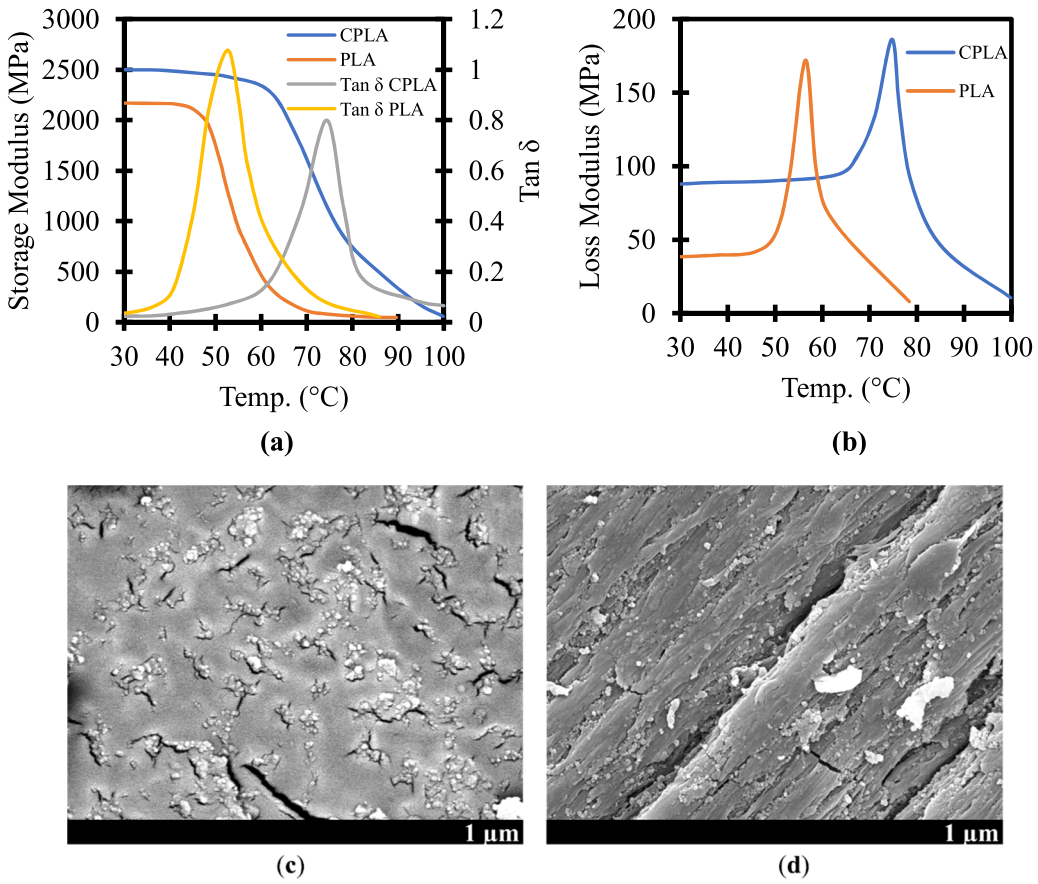

Fig. 5. (a) and (b) DMA traces of CPLA and pure PLA samples. SEM images of a (c) CPLA filament cross-section and (d) 3D-printed CPLA sample.

microstructure of CPLA and show how carbon particles are distributed. As seen in Fig. 5(c) and (d), SEM images of CPLA filament and structure reveal that carbon particles are consistently dispersed throughout the PLA matrix, which is important for the conductivity property.

The early investigations look at the heating capabilities of 4D-printed CPLA traces and the voltage needed for fast activation and heating. With the help of this measurement, the required voltage to stimulate the structures is determined. Three 3D-printed U-shape specimens are connected and heated using voltages of 60 V, 90 V, and 120 V as shown in Fig. 6(a). The resistance changes versus temperature are recorded accordingly (see Fig. 6(b)). Recorded data show increasing temperature and voltage result in higher resistance. When the structure is heated and cooled, an infrared camera records the temperature changes. The temperature growth over time at various voltages is depicted in Fig. 6(c), (d), and (e).

The structure is heated up to 99 °C in 17 s using 120 V. The temperature does not reach T_g using 60 V. Results show that increasing the temperature results in a drop in current over time. This leads to higher resistance and the resistance goes down by cooling the structure [49]. With a higher voltage, the maximum temperature reached rises as expected [60]. After applying the voltage, the CPLA structures reach a temperature plateau, and an equilibrium is formed between the energy supplied by Joule heating and the energy lost to the environment. The specimen is heated faster and results in a lower Young's modulus by 120 V. Due to the requirement for a fast response, 120 V voltage is considered in this study.

Factors impacting the electroactive shape memory performance of printed structures are more complex than those affecting filaments. The thermal characteristics of the printed structures are not significantly impacted by the printing process. But the printed structures' storage modulus marginally declined [29]. The structure has a thickness of 1 mm and consists of five identical single layers. The two long legs of the U-shaped structure, which bend perpendicular to the board surface, are the principal deformation components.

Theoretically, overall energization can be achieved by connecting electrodes at the edges of the U-shaped structure's two long legs. However, the current primarily passes through the interior of the structure with the shortest distance, and the temperature rises in other parts primarily depending on the heat diffusion from this area. As a result, the structure's thermal conductivity along the direction perpendicular to the two long legs is lower than expected. Meanwhile, due to the short width of the structure, this issue is eliminated. Fig. 7(a) displays U-shaped structures' electroactive shape memory capabilities, and the picture of their internal heat distribution is shown in Fig. 7(b). The most even internal heat distribution and activation voltage are found in the specimen due to the concentric pattern and small sizes. The timing of shape recovery shows the 4D-printed structure can achieve its original shape in less than 17 s. The tip bending angle versus time in shape recovery is shown in Fig. 7(c). Also, Fig. 7(d) illustrates the tip bending angle versus temperature accordingly. The results show that the structure goes back to its initial form as soon as the temperature passes the T_g.

3.2. MRE-based composite actuator

Following the polymerization of the resin mixture, as illustrated in Fig. 8(a), it is observed that UF-S2 particles can produce a composite when added to the silicone resin. Magnetization curves are utilized to evaluate the particle-filled silicones' magnetic response. The magnetic moment is up to 0.3 T, which is a low value typically achieved under external magnetic fields. Fig. 8(b) displays the composite film's magnetization moment. The area of the hysteresis loop correlates with the amount of energy dissipated when the field is reversed. The

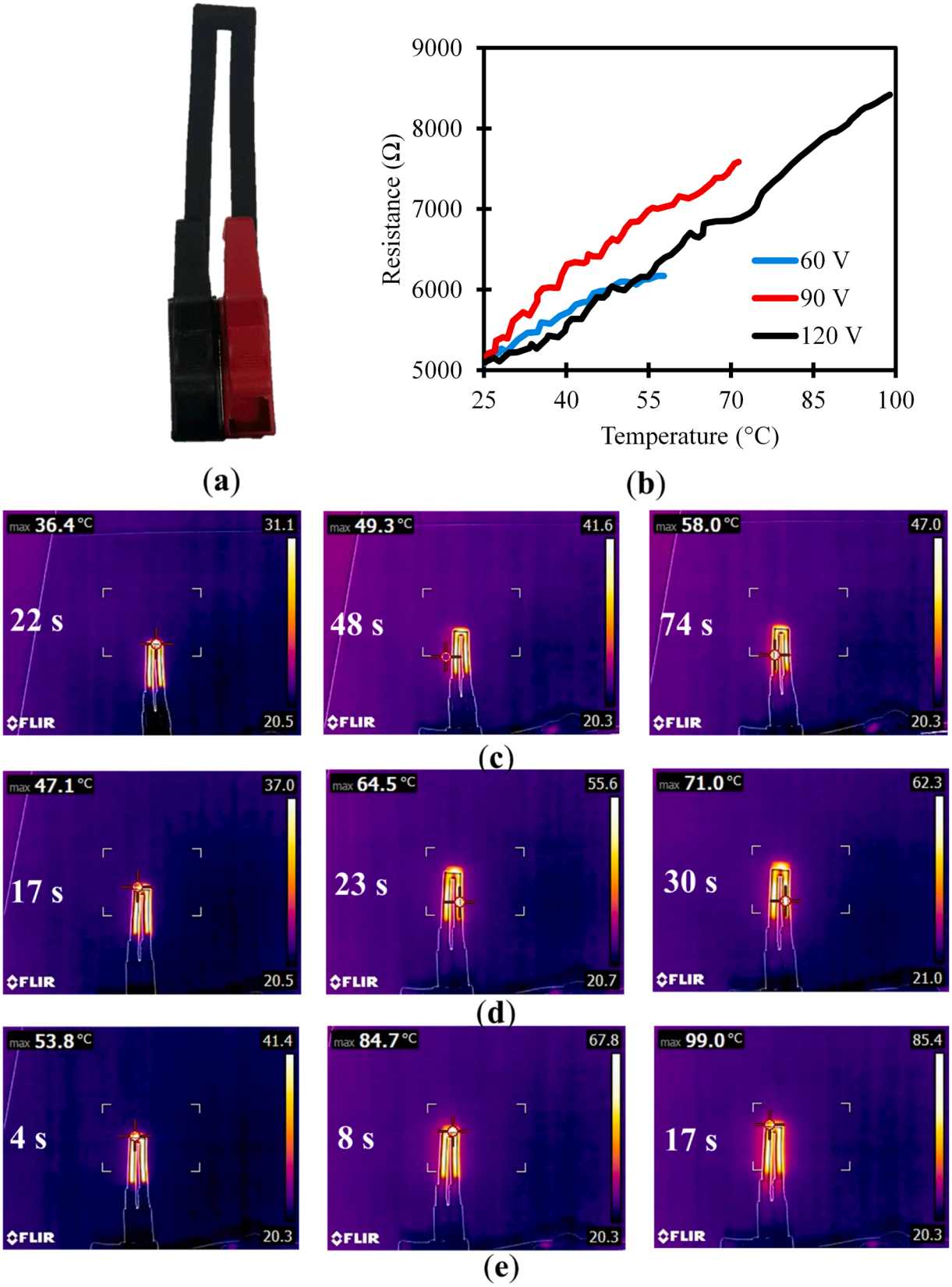

Fig. 6. (a) Clamping of U-shape structure by the crocodile clipper. (b) Resistance changes as the temperature is raised using 60 V, 90 V, and 120 V DC power supply. The U-shaped structure's heat distribution during energization using (c) 60 V, (d) 90 V, and (e) 120 V.

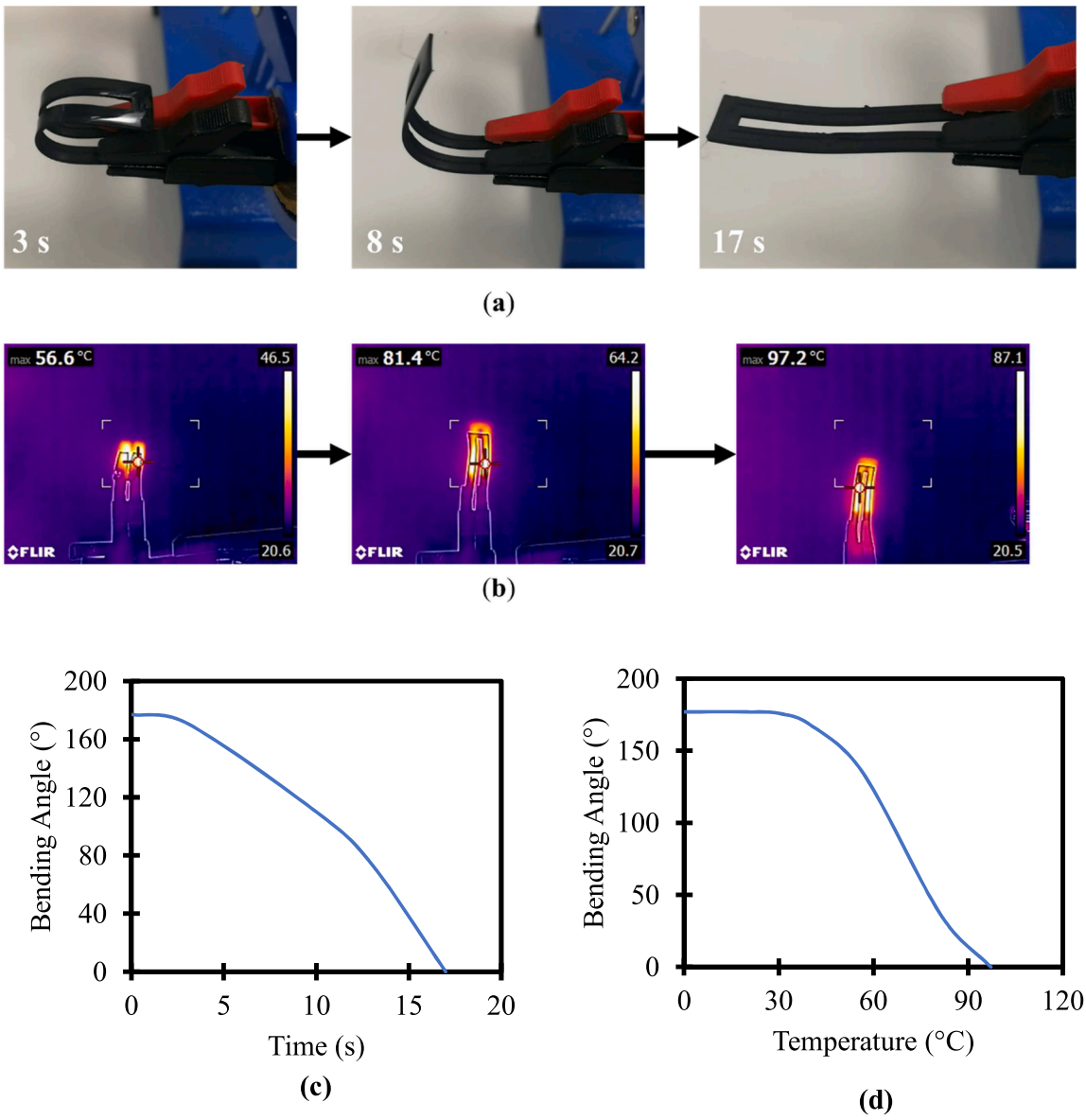

Fig. 7. (a) U-shaped structure with concentric infill pattern electroactive shape recovery procedures using 120 V. (b) The structure heat distribution maps throughout the electroactive shape recovery procedure. (c) The tip bending angle versus time in CPLA shape recovery. (d) The tip bending angle versus temperature in CPLA shape recovery.

saturation magnetization of 30 emu/g, the remanence of 10 emu/g, and the coercivity of 0.02 T are conducted accordingly.

The remanent magnetizations show that the magnetic dipoles of UF-S2 particles are more easily directed when magnetic fields are applied and can be retained after the fields are removed. In order to permanently orient magnetic dipoles in one direction, the external field must be stronger than the coercive magnetic field of the material [47]. This reveals that the particles align with their simple long axis parallel to the applied magnetic field while the resin is still fully curing. The composite films can be activated repeatedly without losing magnetization if the driving field is kept within the capabilities of common permanent magnets.

Moreover, tensile tests also demonstrate that silicone films containing UF-S2 particles perform better than pure silicone films due to their higher compliance (see Fig. 8(c)). The median of five samples is chosen for both pure silicone and silicone with magnetic particles. In contrast to the dog-bone pure silicone samples, the composite films with UF-S2 particles are stronger as a result of the presence of UF-S2 particles.

The following comparison study demonstrates how the structure with the same weight enhances the stability of the magnetic elastomer. In line with this, composite actuators containing 4D-printed structures and without 4D-printed structures are studied. The samples have the same weight and size. Fig. 9(a) and (b) show that the MRE has higher stability when the actuator contains a 4D-printed structure as a core. The MRE lacks sufficient stability with an elastomer thickness of 2.5 mm. This aids in the accuracy and repeatability of actuators. Additionally, reducing weight has positive effects on material waste and lighter products.

An image of the local flux density, which alters linearly with the magnetization of the MRE composite actuator, is presented. Fig. 9(c) demonstrates that the end of the MRE-based composite has a higher concentration of UF-S2 particles. The actuator's magnetization during the curing process is the cause of the negative value. The end of the actuator displays slightly stronger magnetization than the rest of it due to the naturally occurring concentration of magnetic flux near the edges of the magnetising magnet. As a result, the actuator's end is stimulated by a less magnetic field.

The composite actuator is affected in line with low magnetic

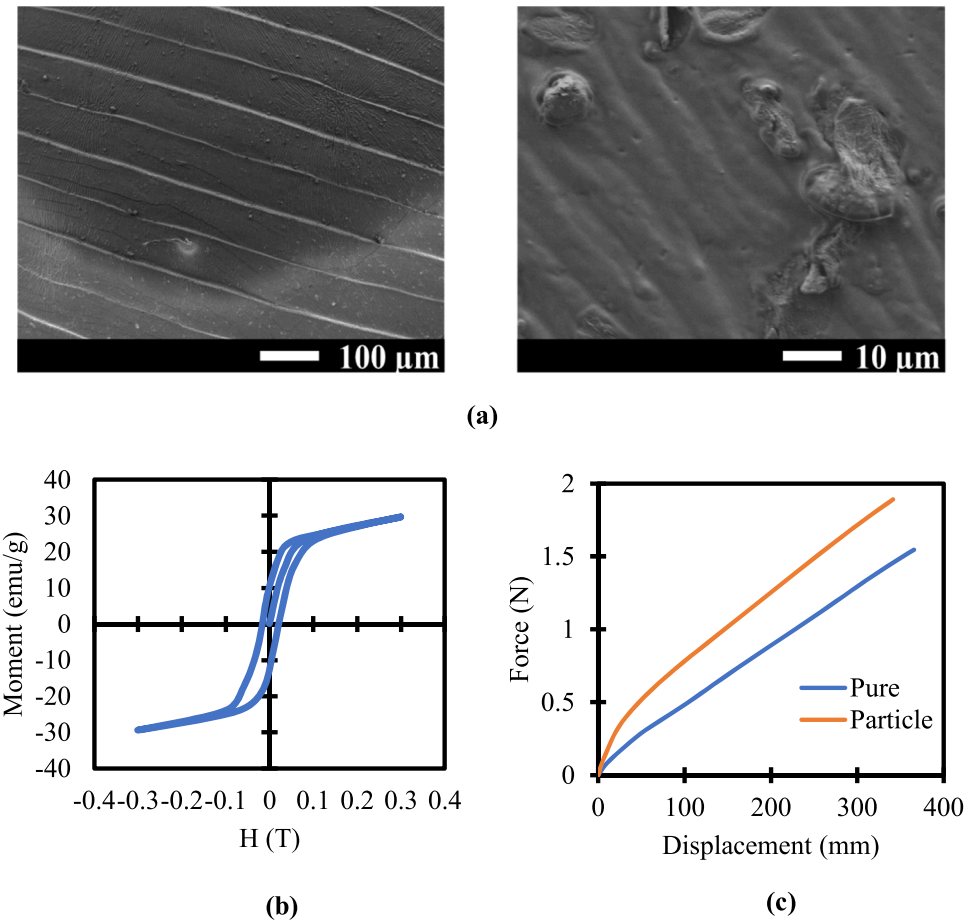

Fig. 8. (a) The SEM images of the shape and size distribution of the UF-S2 particles inside the silicone. (b) H-field cyclic magnetization curve for silicone composites, rising gradually from − 0.3 to 0.3 T. (c) Median of five samples obtained from the tensile test for silicone composite samples containing and excluding magnetic particles.

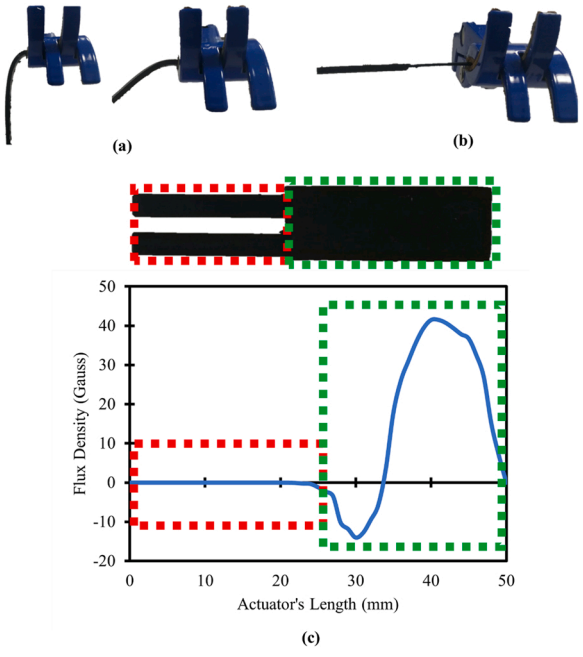

Fig. 9. (a) MRE composites with 50- and 30-mm lengths. (b) MRE-based composite actuator with 4D-printed structure. (c) Composite actuator's magnetic flux density of UF-S2 particles throughout the actuator's length.

strength. According to deflection measurements, the actuation of our composite films is currently possible with external fields that are one order of magnitude lower than the demagnetization limit. One side of the actuator is clamped due to the significant force that the magnetic field produces as shown in Fig. 10(a). The procedure of stimulating the actuator is started by heating it. The electrical current passes the actuator and heats it quickly. The structure's storage modulus decreases and the magnet attracts the actuator as illustrated in Fig. 10(b). The actuator is bent to be aligned with the magnetic field (see Fig. 10(c)). The power supply is turned off and the actuator is cooled at room temperature. The actuator remains in a bent position and the magnetic field is removed accordingly (see Fig. 10(d)). This happens due to the strength and stiffness of the CPLA structure. The actuator becomes stable in the bending situation if required. Meanwhile, the composite actuator goes back to its original form via Joule heating. The 4D-printed structure is heated and returns the actuator to its initial shape as shown in Fig. 10(e) and (f). The heat distribution of the actuator in the attraction procedure is exhibited in Fig. 10(g).

As shown in Fig. 11(a) and (b), the presence of the magnet at the end of the actuator conducts a bi-directional actuator. This occurs as a result of the magnetic domains at the ends of the actuator being oriented in opposition to one another. The actuator's exposure to the closing flux lines connecting the diametrically opposed poles of the magnet pair placements causes this pattern to form. The magnetic field along these closing lines is oriented in the opposite direction from the magnetic field generated at the composite actuator's end. This feature helps to increase the shape recovery time faster. The actuator in the bending position is heated and the permanent magnet is rotated accordingly. As soon as the

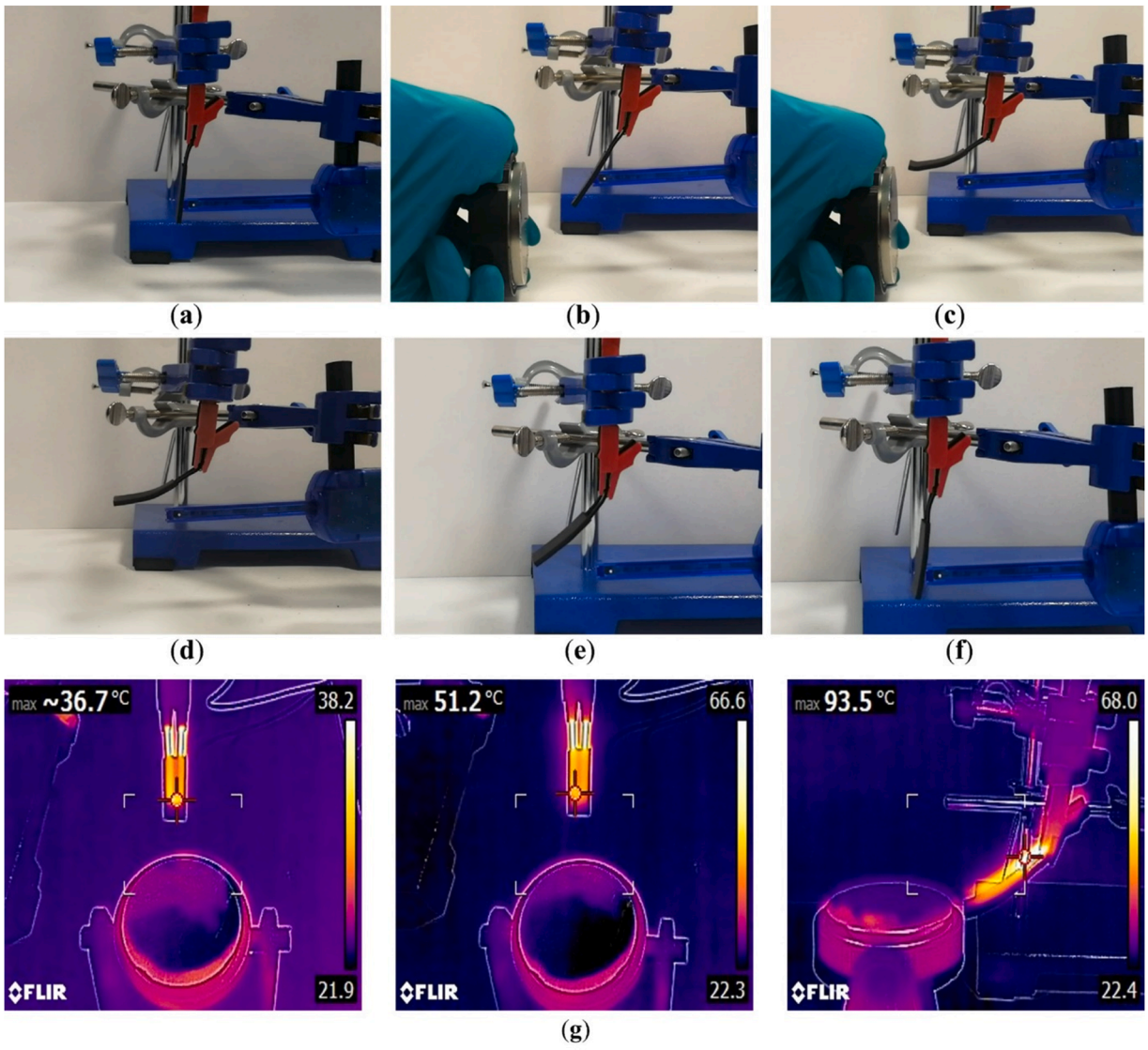

Fig. 10. (a) Composite actuator holding in vertical position. (b) Joule heating and bringing the magnet close to the composite. (c) Reaching maximum temperature and bending angle via magnetic attraction. (d) The composite actuator remains in its position by removing the permanent magnet. (e) Turning power on to heat the composite actuator. (f) The composite actuator goes back to its original shape using Joule heating in 18 s (g) Heat dispersion throughout the energization and attraction processes of the actuator.

actuator reaches T_g, the magnet starts to repulse the composite actuator. The obtained data show that the actuator is bi-stable since it can remain in two different shapes using Joule heating and magnetic field stimuli.

The response of the composite actuator to an external magnetic field reflects the magnetic and mechanical properties that have been observed. Due to their high compliance and magnetism, actuator containing UF-S2 demonstrates outstanding magneto-responsiveness in the presence of magnetic fields. Throughout the process, the magnetic field strength is also recorded. By reducing the distance between the magnets, the magnetic field's axial strength increases. The trajectory pathways of composite actuators demonstrate how the magnet attracts and repels the composite actuator, as shown in Fig. 11(c). The axial strength measurement for attraction is 18 mT. Also, the value of 34 mT is obtained by rotating the magnet. The field strength in repulsion is higher because the magnet is closer to the actuator. The maximum bending angle of attraction is 80° and for repulsion is 76°. The results indicate the possibility to programme and control the actuator remotely.

This observation indicates that the 4D-printed structure is very successful in improving the MRE's performance as an actuator. Additionally, depending on the requirements and magnetic field intensity, this concept may be used with various designs and forms. To assess the actuator's cyclic behaviour, a single actuator undergoes a 200-cycle fatigue test. The current is regulated on and off using a relay switch. The dynamic behaviour is constrained by the system's cooling since CPLA has temperature-dependent effects. In order to assess changes after 200 repetitions, the temperature is also recorded using a thermometer. The findings show that the temperature has remained consistent and has not altered (see Fig. 11(d)). Also, the MRE composite shows a good bonding interaction with the 4D-printed structure after the cycling test. Meanwhile, a further rise in temperatures beyond 100 °C results in the melting of the CPLA structure. Fig. 11(e) illustrates the stages of the actuator's tip angle in both repulsion and attraction over the magnetic field strength. Since the magnet gets closer to the actuator the field, strength and angle increase simultaneously. Also, Fig. 11(f) and (g) show the shape recovery of the deflected actuator over time and temperature. The actuator goes back to its initial form after T_g in 18 s. The shape recovery percentage of attracted and repulsed actuators are shown in Fig. 11(h).

A bi-stable form is easier to produce with two stimuli than just temperature and magnet alone. The structure can be just attracted in the proper position alone without locking by the magnetic field.

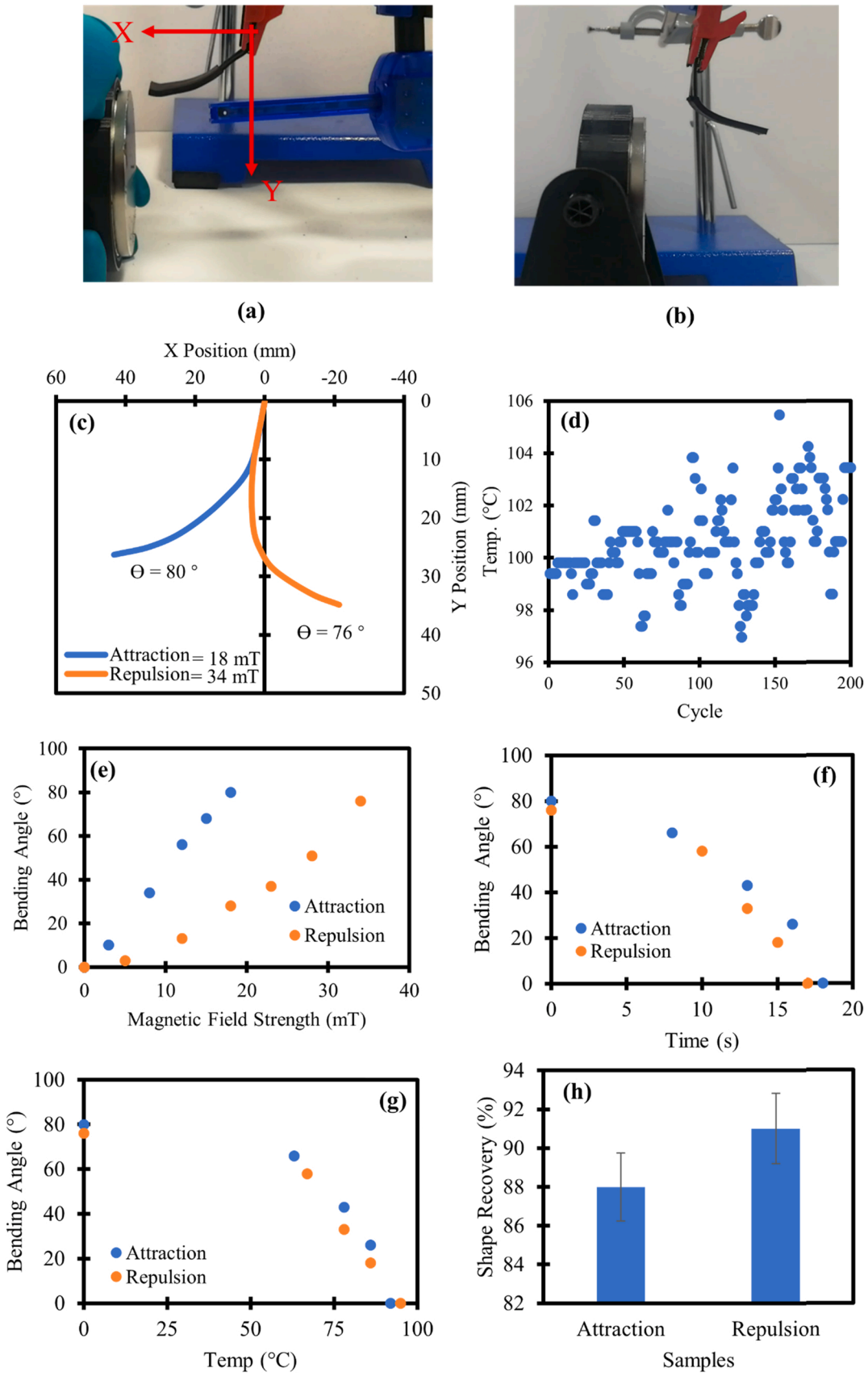

Fig. 11. (a) Attraction deflection of the actuator. (b) Repulsion deflection of the actuator. (c) The trajectory deflection of the actuator in the attraction and repulsion procedure with the maximum bending angle. (d) Temperature fatigue cycling test. (e) The tip bending angle of the actuator in attraction and repulsion conditions versus magnetic field strength. (f) Shape recovery tip bending angle over time in attraction and repulsion conditions. (g) Shape recovery tip bending angle over temperature. (h) Shape recovery rate in both attraction and repulsion conditions.

Additionally, it is unable to produce new shapes with just Joule heating because as the structure's temperature rises, it tends to recover its original shape. Meanwhile, combining the two stimuli enables us to create highly solid and multiple forms.

3.3. Potential applications

This section aims to illustrate the possible usage of MRE-based electroactive composite actuators for mechanical and biomedical engineering applications. For instance, grippers can be designed using this composite actuator. After Joule heating and attracting the actuator using a magnetic field, the deflected actuator is cooled at room temperature. Then, the magnetic field is removed, and the actuator maintains its position accordingly. In deflected position, the load weights are applied to the actuator, and it can grasp and hold as shown in Fig. 12(a). The actuator with a weight of 1.47 g can hold and lift weights up to 200 g. Changing the design and developing a larger actuator with this technique can increase the lifting capabilities. Also, an assembly of this actuator can be used as a gripper to pick-and-place different objects of various shapes. The advantage of the gripper is that it can maintain the grasping position for a long time without using magnetic fields or any other stimuli.

The bi-directional feature of this actuator allows for modifying the structure during the Joule heating based on requirements. The actuator can be controlled by a magnet to achieve various shapes and used as an attachment-like hook mechanism inside a system. A 3D-printed structure is used here to show the capability of the composite actuator as a remotely controlled hook. The actuator can be used inside the structure and bent to reach a target spot which is difficult to reach. The heating procedure by the electrical system is performed. The magnetic field is then used to repulse and bend the actuator accordingly. The actuator is bent and works as a hook to hold or lock itself to the system or object. The actuator is then cooled and stayed in deflected position as long as required (see Fig. 12(b)). It may be utilised in biomedical devices for a variety of supportive functions, including tracheal splints and shattered bones. A self-deployable stent may be another excellent use for such a magneto-responsive electroactive actuator. Due to the capability of the actuator, the smaller size of this could be used in human vessels to treat blood clots in vessels.

Also, the potential application of 4D-printed constructions is to be used as a hook mechanism. The concept is the actuator can be bent and locked by controlling it remotely. The actuator can be used as a locking system to lock and open due to the bi-stability and shape memory behaviour. The 4D structure may be used for individualised locking systems since it can be controlled remotely. Fig. 12(c) depicts a concept of the 4D structure's mechanism as a hook-shaped locking system. The adaptive actuator is triggered when the temperature rises over the critical temperature and a magnetic field is applied. The actuator is repulsed or attracted and bent which closes the system. Two sets of these actuators can be worked as a locker in a system. The examples used in this study are only a few of the many applications that the 4D-printed CPLA/UF-S2 composite actuator can possess. This adaptable element has the potential to be employed as flexible and conformal parts for future mechanical and biological devices created using 4D printing technology.

4. Conclusion

In the current study, a simple process for creating MRE-based electroactive shape memory structures using FDM and silicone casting was introduced. First, the CPLA filament was examined as the primary core structure. Joule heating and shape recovery of the 4D-printed structure were investigated. The filament's electrical, thermal, and electroactive shape memory characteristics were identified using different input voltages. The stability of MRE-based actuators was increased by 4DP technology. Controlling remotely and programming the composite actuator were also determined. The method of shape recovery at a given temperature and magnetic field was described. It was possible to regulate the actuator using a weak magnetic field. In terms of microstructure, shape recovery, and dual stimuli, the unique composite actuator was

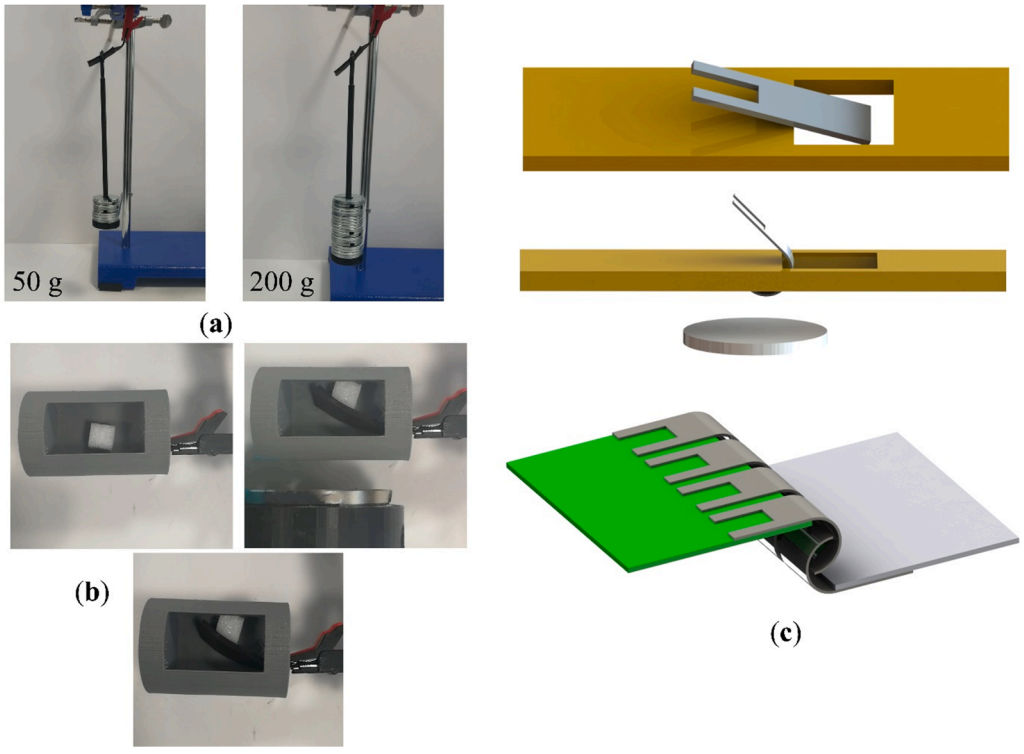

Fig. 12. (a) Holding different weights after programming and cooling the actuator. (b) Stimulating a hook-like actuator in a closed system inside the structure. (c) An illustration of the actuator's mechanism as a hook in locking and releasing systems.

examined. It was discovered that the 4D-printed CPLA was rapid enough to return to its original shape using a 120 V power supply. For the composite actuator, a maximum bending angle of 80° for attraction and 76° for repulsion was attained with low external fields. The actuator capabilities in terms of being bi-directional and bi-stable were examined. The cycling test showed that the actuator can work without issues in long-term procedures. It was experimentally revealed that the composite actuators created with 4DP and MRE have great potential in mechanical/biomedical applications like a lifter, locker, and biomedical sectors. This research is likely to advance the state-of-the-art 4DP and unlock potential in the design and development of functional structures with bi-stable/bi-directional and shape recovery features in a controllable manner.

CRediT authorship contribution statement

M. Lalegani Dezaki: Conceptualization, Data curation, Validation, Visualization, Methodology, Investigation, Formal analysis, Writing – original draft, Writing – review & editing. **M. Bodaghi:** Conceptualization, Methodology, Investigation, Formal analysis, Writing – review & editing, Director of Study.

Declaration of Competing Interest

The authors declare that they have no known competing financial interests or personal relationships that could have appeared to influence the work reported in this paper.

Data Availability

Data will be made available on request.

References

[1] C.A. Spiegel, M. Hackner, V.P. Bothe, J.P. Spatz, E. Blasco, 4D Printing of Shape Memory Polymers: From Macro to Micro, Adv. Funct. Mater. (2022), https://doi.org/10.1002/adfm.202110580.

[2] M. Bodaghi, A.R. Damanpack, W.H. Liao, Self-expanding/shrinking structures by 4D printing, Smart Mater. Struct. 25 (2016), https://doi.org/10.1088/0964-1726/25/10/105034.

[3] M. Bodaghi, A.R. Damanpack, W.H. Liao, Adaptive metamaterials by functionally graded 4D printing, Mater. Des. 135 (2017), https://doi.org/10.1016/j.matdes.2017.08.069.

[4] C. Lin, L. Liu, Y. Liu, J. Leng, 4D printing of shape memory polybutylene succinate/polylactic acid (PBS/PLA) and its potential applications, Compos Struct. 279 (2022), https://doi.org/10.1016/j.compstruct.2021.114729.

[5] M. Barletta, A. Gisario, M. Mehrpouya, 4D printing of shape memory polylactic acid (PLA) components: Investigating the role of the operational parameters in fused deposition modelling (FDM), J. Manuf. Process 61 (2021), https://doi.org/10.1016/j.jmapro.2020.11.036.

[6] A. Zolfagharian, M.A.P. Mahmud, S. Gharaie, M. Bodaghi, A.Z. Kouzani, A. Kaynak, 3D/4D-printed bending-type soft pneumatic actuators: fabrication, modelling, and control, Virtual Phys. Prototyp. 15 (2020) 373–402, https://doi.org/10.1080/17452759.2020.1795209.

[7] Z. Zhang, K.G. Demir, G.X. Gu, Developments in 4D-printing: a review on current smart materials, technologies, and applications, Int J. Smart Nano Mater. 10 (2019), https://doi.org/10.1080/19475411.2019.1591541.

[8] S.K. Leist, J. Zhou, Current status of 4D printing technology and the potential of light-reactive smart materials as 4D printable materials, Virtual Phys. Prototyp. 11 (2016), https://doi.org/10.1080/17452759.2016.1198630.

[9] T. Mu, L. Liu, X. Lan, Y. Liu, J. Leng, Shape memory polymers for composites, Compos Sci. Technol. 160 (2018), https://doi.org/10.1016/j.compscitech.2018.03.018.

[10] M. Lalegani Dezaki, M. Bodaghi, A. Serjouei, S. Afazov, A. Zolfagharian, Adaptive reversible composite-based shape memory alloy soft actuators, Sens Actuators A Phys. 345 (2022), 113779, https://doi.org/10.1016/j.sna.2022.113779.

[11] Y. Xia, Y. He, F. Zhang, Y. Liu, J. Leng, A review of shape memory polymers and composites: mechanisms, materials, and applications, Adv. Mater. 33 (2021), https://doi.org/10.1002/adma.202000713.

[12] E. Yarali, M. Baniasadi, A. Zolfagharian, M. Chavoshi, F. Arefi, M. Hossain, A. Bastola, M. Ansari, A. Foyouzat, A. Dabbagh, M. Ebrahimi, M.J. Mirzaali, M. Bodaghi, Magneto-/ electro-responsive polymers toward manufacturing, characterization, and biomedical/ soft robotic applications, Appl. Mater. Today 26 (2022), 101306, https://doi.org/10.1016/j.apmt.2021.101306.

[13] S. Petsch, R. Rix, B. Khatri, S. Schuhladen, P. Müller, R. Zentel, H. Zappe, Smart artificial muscle actuators: Liquid crystal elastomers with integrated temperature feedback, Sens Actuators A Phys. 231 (2015), https://doi.org/10.1016/j.sna.2014.10.014.

[14] M. Askari, M. Afzali Naniz, M. Kouhi, A. Saberi, A. Zolfagharian, M. Bodaghi, Recent progress in extrusion 3D bioprinting of hydrogel biomaterials for tissue regeneration: A comprehensive review with focus on advanced fabrication techniques, Biomater. Sci. 9 (2021), https://doi.org/10.1039/d0bm00973c.

[15] M. Bodaghi, A. Serjouei, A. Zolfagharian, M. Fotouhi, H. Rahman, D. Durand, Reversible energy absorbing meta-sandwiches by FDM 4D printing, Int J. Mech. Sci. 173 (2020), https://doi.org/10.1016/j.ijmecsci.2020.105451.

[16] A. Nishiguchi, H. Zhang, S. Schweizerhof, M.F. Schulte, A. Mourran, M. Möller, 4D printing of a light-driven soft actuator with programmed printing density, ACS Appl. Mater. Interfaces 12 (2020), https://doi.org/10.1021/acsami.0c02781.

[17] A. Muzaffar, M.B. Ahamed, K. Deshmukh, T. Kovářík, T. Křenek, S.K.K. Pasha, 3D and 4D printing of pH-responsive and functional polymers and their composites, 3D 4D Print. Polym. Nanocompos. Mater.: Process. Appl. Chall. (2019), https://doi.org/10.1016/B978-0-12-816805-9.00004-1.

[18] H. Böse, T. Gerlach, J. Ehrlich, Magnetorheological elastomers — an underestimated class of soft actuator materials, J. Intell. Mater. Syst. Struct. 32 (2021), https://doi.org/10.1177/1045389×21990888.

[19] Q. Zheng, C. Xu, Z. Jiang, M. Zhu, C. Chen, F. Fu, Smart actuators based on external stimulus response, Front Chem. 9 (2021), https://doi.org/10.3389/fchem.2021.650358.

[20] T. Cheng, M. Thielen, S. Poppinga, Y. Tahouni, D. Wood, T. Steinberg, A. Menges, T. Speck, Bio-inspired motion mechanisms: computational design and material programming of self-adjusting 4D-printed wearable systems, Adv. Sci. 8 (2021), https://doi.org/10.1002/advs.202100411.

[21] M.Y. Khalid, Z.U. Arif, W. Ahmed, R. Umer, A. Zolfagharian, M. Bodaghi, 4D printing: technological developments in robotics applications, Sens Actuators A Phys. 343 (2022), 113670, https://doi.org/10.1016/j.sna.2022.113670.

[22] J. Carrell, G. Gruss, E. Gomez, Four-dimensional printing using fused-deposition modeling: a review, Rapid Prototyp. J. 26 (2020), https://doi.org/10.1108/RPJ-12-2018-0305.

[23] M. Lalegani Dezaki, M.K.A. Mohd Ariffin, S. Hatami, An overview of fused deposition modelling (FDM): research, development and process optimisation, Rapid Prototyp. J. 27 (2021) 562–582, https://doi.org/10.1108/RPJ-08-2019-0230.

[24] A. Cano-Vicent, M.M. Tambuwala, S.S. Hassan, D. Barh, A.A.A. Aljabali, M. Birkett, A. Arjunan, Á. Serrano-Aroca, Fused deposition modelling: Current status, methodology, applications and future prospects, Addit. Manuf. 47 (2021), https://doi.org/10.1016/j.addma.2021.102378.

[25] H. Lu, M. Lei, C. Zhao, B. Xu, J. Leng, Y.Q. Fu, Structural design of flexible Au electrode to enable shape memory polymer for electrical actuation, Smart Mater. Struct. 24 (2015), https://doi.org/10.1088/0964-1726/24/4/045015.

[26] M.Y. Razzaq, M. Anhalt, L. Frormann, B. Weidenfeller, Thermal, electrical and magnetic studies of magnetite filled polyurethane shape memory polymers, Mater. Sci. Eng. A. 444 (2007), https://doi.org/10.1016/j.msea.2006.08.083.

[27] I.T. Garces, C. Ayranci, Advances in additive manufacturing of shape memory polymer composites, Rapid Prototyp. J. 27 (2021), https://doi.org/10.1108/RPJ-07-2020-0174.

[28] H. Meng, G. Li, A review of stimuli-responsive shape memory polymer composites, Polym. (Guildf.) 54 (2013) 2199–2221, https://doi.org/10.1016/j.polymer.2013.02.023.

[29] X. Dong, F. Zhang, L. Wang, Y. Liu, J. Leng, 4D printing of electroactive shape-changing composite structures and their programmable behaviors, Compos Part A Appl. Sci. Manuf. 157 (2022), https://doi.org/10.1016/j.compositesa.2022.106925.

[30] R. Mitkus, F. Cerbe, M. Sinapius, 2 - 4D printing electro-induced shape memory polymers, in: M. Bodaghi, A. Zolfagharian (Eds.), Smart Materials in Additive Manufacturing, Elsevier, 2022, pp. 19–51, https://doi.org/10.1016/B978-0-323-95430-3.00002-6.

[31] G. Wang, T. Cheng, Y. Do, H. Yang, Y. Tao, J. Gu, B. An, L. Yao, Printed paper actuator: a low-cost reversible actuation and sensing method for shape changing interfaces, Conf. Hum. Factors Comput. Syst. - Proc. (2018), https://doi.org/10.1145/3173574.3174143.

[32] Y.C. Lee Y.S. Alshebly M. Nafea Joule Heating Activation of 4D Printed Conductive PLA Actuators 2022 IEEE Int. Conf. Autom. Control Intell. Syst. (I2CACIS), IEEE 2022 221 225 doi: 10.1109/I2CACIS54679.2022.9815495.

[33] P.F. Flowers, C. Reyes, S. Ye, M.J. Kim, B.J. Wiley, 3D printing electronic components and circuits with conductive thermoplastic filament, Addit. Manuf. 18 (2017) 156–163, https://doi.org/10.1016/j.addma.2017.10.002.

[34] M. Li, A. Pal, A. Aghakhani, A. Pena-Francesch, M. Sitti, Soft actuators for real-world applications, Nat. Rev. Mater. 7 (2022), https://doi.org/10.1038/s41578-021-00389-7.

[35] J. Bernat, P. Gajewski, R. Kapela, A. Marcinkowska, P. Superczyńska, Design, fabrication and analysis of magnetorheological soft gripper, Sensors 22 (2022) 2757, https://doi.org/10.3390/s22072757.

[36] H. Chung, A.M. Parsons, L. Zheng, Magnetically controlled soft robotics utilizing elastomers and gels in actuation: a review, Adv. Intell. Syst. 3 (2021), https://doi.org/10.1002/aisy.202000186.

[37] A.G. Díez, C.R. Tubio, J.G. Etxebarria, S. Lanceros-Mendez, Magnetorheological elastomer-based materials and devices: state of the art and future perspectives, Adv. Eng. Mater. 23 (2021), https://doi.org/10.1002/adem.202100240.

[38] C. Khazoom, P. Caillouette, A. Girard, J.S. Plante, A supernumerary robotic leg powered by magnetorheological actuators to assist human locomotion, IEEE Robot Autom. Lett. 5 (2020), https://doi.org/10.1109/LRA.2020.3005629.

[39] S. Kashima, F. Miyasaka, K. Hirata, Novel soft actuator using magnetorheological elastomer, IEEE Trans. Magn. 48 (2012), https://doi.org/10.1109/TMAG.2011.2173669.
[40] H. Böse, R. Rabindranath, J. Ehrlich, Soft magnetorheological elastomers as new actuators for valves, J. Intell. Mater. Syst. Struct. (2012), https://doi.org/10.1177/1045389×11433498.
[41] W. Hu, G.Z. Lum, M. Mastrangeli, M. Sitti, Small-scale soft-bodied robot with multimodal locomotion, Nature 554 (2018), https://doi.org/10.1038/nature25443.
[42] T. Xu, J. Zhang, M. Salehizadeh, O. Onaizah, E. Diller, Millimeter-scale flexible robots with programmable three-dimensional magnetization and motions, Sci. Robot 4 (2019), https://doi.org/10.1126/scirobotics.aav4494.
[43] Y. Kim, H. Yuk, R. Zhao, S.A. Chester, X. Zhao, Printing ferromagnetic domains for untethered fast-transforming soft materials, Nature 558 (2018), https://doi.org/10.1038/s41586-018-0185-0.
[44] D. Tang, C. Zhang, H. Sun, H. Dai, J. Xie, J. Fu, P. Zhao, Origami-inspired magnetic-driven soft actuators with programmable designs and multiple applications, Nano Energy 89 (2021), https://doi.org/10.1016/j.nanoen.2021.106424.
[45] J. Zhang, O. Onaizah, K. Middleton, L. You, E. Diller, Reliable grasping of three-dimensional untethered mobile magnetic microgripper for autonomous pick-and-place, IEEE Robot Autom. Lett. 2 (2017), https://doi.org/10.1109/LRA.2017.2657879.
[46] V. Skfivan, O. Sodomka, F. Mach, Magnetically guided soft robotic grippers, in: Proceedings ofRoboSoft 2019 - 2019 IEEE International Conference on Soft Robotics, 2019. ⟨https://doi.org/10.1109/ROBOSOFT.2019.8722762⟩.
[47] J.A. Carpenter, T.B. Eberle, S. Schuerle, A. Rafsanjani, A.R. Studart, Facile manufacturing route for magneto-responsive soft actuators, Adv. Intell. Syst. 3 (2021) 2000283, https://doi.org/10.1002/aisy.202000283.
[48] H. Iwasaki, F. Lefevre, D.D. Damian, E. Iwase, S. Miyashita, Autonomous and reversible adhesion using elastomeric suction cups for in-vivo medical treatments, IEEE Robot Autom. Lett. 5 (2020), https://doi.org/10.1109/LRA.2020.2970633.
[49] M. Al-Rubaiai, T. Pinto, D. Torres, N. Sepulveda, X. Tan, Characterization of a 3D-printed conductive PLA material with electrically controlled stiffness, in: Development and Characterization of Multifunctional Materials; Mechanics and Behavior of Active Materials; Bioinspired Smart Materials and Systems; Energy Harvesting; Emerging Technologies, Volume 1, American Society of Mechanical Engineers, 2017, https://doi.org/10.1115/SMASIS2017-3801.
[50] M.L. Dezaki, M. Bodaghi, Soft magneto-responsive shape memory foam composite actuators, Macromol. Mater. Eng. (2022) 2200490, https://doi.org/10.1002/mame.202200490.
[51] H. Tripathi, G.C. Pandey, A. Dubey, S.K. Shaw, N.K. Prasad, S.P. Singh, C. Rath, Superparamagnetic manganese ferrite and strontium bioactive glass nanocomposites: enhanced biocompatibility and antimicrobial properties for hyperthermia application, Adv. Eng. Mater. 23 (2021) 2000275, https://doi.org/10.1002/adem.202000275.
[52] A. de Oliveira Barros, M.N. Hasan Kashem, D. Luna, W.J. Geerts, W. Li, J. Yang, Magnetic properties of PDMS embedded with strontium ferrite particles cured under different magnetic field configurations, AIP Adv. 12 (2022), 035121, https://doi.org/10.1063/9.0000338.
[53] R. Stopforth, Conductive polylactic acid filaments for 3D printed sensors: experimental electrical and thermal characterization, Sci. Afr. 14 (2021), https://doi.org/10.1016/j.sciaf.2021.e01040.
[54] J. Beniak, Ľ. Šooš, P. Križan, M. Matúš, V. Ruprich, Resistance and strength of conductive PLA processed by FDM additive manufacturing, Polymers 14 (2022) 678, https://doi.org/10.3390/polym14040678.
[55] Y.C. Lee, Y.S. Alshebly, M. Nafea, Joule heating activation of 4D printed conductive PLA actuators, in: Proceedings of the 2022 IEEE International Conference on Automatic Control and Intelligent Systems (I2CACIS), 2022: pp. 221–225. ⟨ https://doi.org/10.1109/I2CACIS54679.2022.9815495⟩.
[56] G. Ausanio, V. Iannotti, E. Ricciardi, L. Lanotte, L. Lanotte, Magneto-piezoresistance in magnetorheological elastomers for magnetic induction gradient or position sensors, Sens Actuators A Phys. 205 (2014), https://doi.org/10.1016/j.sna.2013.10.009.
[57] M.M. Said, J. Yunas, R.E. Pawinanto, B.Y. Majlis, B. Bais, PDMS based electromagnetic actuator membrane with embedded magnetic particles in polymer composite, Sens Actuators A Phys. 245 (2016), https://doi.org/10.1016/j.sna.2016.05.007.
[58] Q. Ze, X. Kuang, S. Wu, J. Wong, S.M. Montgomery, R. Zhang, J.M. Kovitz, F. Yang, H.J. Qi, R. Zhao, Magnetic shape memory polymers with integrated multifunctional shape manipulation, Adv. Mater. 32 (2020), https://doi.org/10.1002/adma.201906657.
[59] N.N. Azmi, M.N.A. Ab Patar, S.N.A. Mohd Noor, J. Mahmud, Testing standards assessment for silicone rubber, in: 2014 International Symposium on Technology Management and Emerging Technologies, IEEE, 2014: pp. 332–336. ⟨https://doi.org/10.1109/ISTMET.2014.6936529⟩.
[60] I.T. Garces, C. Ayranci, Active control of 4D prints: Towards 4D printed reliable actuators and sensors, Sens Actuators A Phys. 301 (2020), 111717, https://doi.org/10.1016/j.sna.2019.111717.

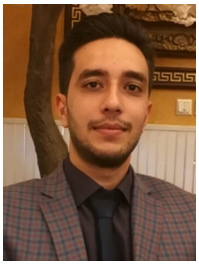

Mohammadreza Lalegani Dezaki received his MSc degree in Manufacturing Systems Engineering from Universiti Putra Malaysia (UPM). He has published several papers in the field of 3D printing and soft actuators. In 2021, He was awarded a PhD Studentship issued by Nottingham Trent University (NTU). His current research interests involve 3D/4D printing and smart soft actuators for soft robots.

Dr Mahdi Bodaghi (B.Sc., M.Sc., Ph.D., PGCAP, FHEA, CEng, MIMechE) is a Senior Lecturer in the Department of Engineering at Nottingham Trent University. He is also the founder and director of the 4D Materials & Printing Lab that hosts a broad portfolio of projects focusing on the electro-thermo-mechanical multi-scale behaviours of smart materials, soft robotics, and 3D/4D printing technologies. His vast experience and research on smart materials and additive manufacturing has led him to co-found the 4D Printing Society and to co-edit the book series- Smart Materials in Additive Manufacturing. His research has also resulted in the publication of over 165 scientific papers in prestigious journals as well as the presentation of his work at major international conferences. Mahdi has also served as Chairman and member of Scientific Committees for 15 International Conferences, as Guest Editor for 10 Journals, as Editorial Board Member for 10 scientific Journals, and as Reviewer for over 150 Journals. Mahdi's research awards include the Best Doctoral Thesis Award of 2015, 2016 CUHK Postdoctoral Fellowship, the Annual Best Paper Award in Mechanics and Material Systems presented by the American Society of Mechanical Engineers in 2017, 2018 Horizon Fellowship Award, and 2021 IJPEM-GT Contribution Award recognized by the Korea Society for Precision Engineering.